ORIGINAL PAPER

Cytotoxicity and Genotoxicity of Biosynthesized Gold and Silver Nanoparticles on Human Cancer Cell Lines

Asra Parveen · Srinath Rao

Abstract Nanoparticles research is currently an area of passionate scientific interest due to its wide variety of potential applications in therapeutic and biomedical interest. This paper presents cytotoxicity and genotoxicity of gold and silver nanoparticles synthesized by using *Cassia auriculata* leaf extract at room temperature on different cancer cell lines. The characterization was performed by UV-Vis spectroscopy, Fourier transform infrared (FTIR) spectroscopy, X-ray diffraction (XRD) and Transmission Electron Measurement (TEM). Cytotoxicity was analyzed against human carcinoma cells lines by MTT assay, while genotoxicity was monitored by agarose gel electrophoresis method. The UV-Vis spectroscopy reveals surface plasmon absorption maxima at 541 nm for gold and 425 nm for silver. The peaks in XRD pattern were in good agreement with the standard values of the face centered cubic form, with an average size of 21 nm in gold and 20 nm in silver. TEM reveals that the particles were spherical and polydisperse. This biological procedure for synthesis of AuNPs and AgNPs and selective inhibition of cancerous cells opens an alternative avenue to treat human cancer effectively. Least concentration of AgNPs was more toxic and AuNPs reveals dose dependent response.

Keywords Nanoparticles · Biological synthesis · Characterization · Cytotoxicity · Genotoxicity

A. Parveen · S. Rao (✉)
Plant Tissue Culture and Genetic Engineering Laboratory, Department of Post Graduate Studies and Research in Botany, Gulbarga University, Gulbarga 585106, Karnataka, India
e-mail: srinathraomm@gmail.com

A. Parveen
e-mail: asrakhateeb11@gmail.com

$\textcircled{\underline{\hspace{0.5em}}}$ Springer

Introduction

Cancer is a leading cause of death worldwide [1] with an estimated prediction of 13.1 million deaths by 2030 [2]. Despite good advancements for diagnosis and treatment, cancer is still a big threat to our society [3]. This is the second most common disease after cardiovascular disorders for maximum deaths in the world [4]. It accounts for about 23 % deaths in USA and 7 % in India. The world's population is expected to be 7.5 billion by 2020 and it has been predicted that approximately 15.0 million new cancer cases would be diagnosed, with deaths of about 12.0 million cancer patients [5]. Approximately 50 % of human cancer treatments are based on chemotherapy. Despite many efforts, multi drug resistance is still considered as a major drawback in chemotherapy of cancer which has been the subject of exhaustive experiments [6]. The cellular mechanisms underlying this phenomenon are well-discussed [7].

Recently, Cancer Nanotechnology is emerged as a promising research domain that can contribute to advanced drug delivery systems, and new ways to diagnose and treat cancer disease or repair damaged tissues and cells [8]. According to a study by the European Science Foundation, there is a need for large investment in developing new nanotechnology based medical tools for diagnostics and therapeutics [9]. Use of transition metals for inorganic nanoparticle based cancer therapeutics is a growing area of interest [10]. There is increasing demand for anticancer therapy [11]. In vitro cytotoxicity testing procedures reduce the use of laboratory animals [12], which has increased the use of cultured tissues and cells [13]. The commercialization of nanoparticles for nanomedicine is also progressing significantly. According to the National Science Foundation, the market size for pharmaceutical nanoproducts would reach approximately US$180 billion per year between 2010 and 2015 [14].

The major merit of biological approach is relatively simple and fast. In addition, it offers high yield, low toxicity, low cost and biocompatibility. Biosynthesized AgNPs from leaf extract of *Vitex negundo* was proved to be an antitumor agent against human colon cancer cell line HCT15 [15]. In vitro cytotoxicity of AgNPs synthesized by *Sesbania grandiflora* leaf extract was analyzed [16] and focused on human breast cancer (MCF-7) and silver nanoparticles synthesized from calli extract of *Citrullus colocynthis* was investigated [17] for human epidermoid larynx carcinoma cell line. Govender et al. 2013 [18] studied cytotoxic activity of *Albizia adianthifolia* (AA)-mediated silver nanoparticles and showed the activation of AA AgNP in the intrinsic apoptotic pathway in A549 lung carcinoma cells. Gold nanoparticles synthesized from grapes extract showed anticancer activity against HeLa cell lines [19]. Green synthesis of gold and silver nanoparticles using leaves extract and cytotoxic effects on different cell lines are well documented [20–24]. Cancer cells, for instance, are more resilient towards nanoparticle toxicity than normal cells due to an increased rate of proliferation and metabolic activity [25]. It was also suggested that silver ions (particularly Ag^+) released from silver nanoparticles could interact with phosphorus moieties in DNA, resulting in inactivation of DNA replication, or react with sulfur-containing proteins, leading to the inhibition of enzyme functions, which results in loss of cell viability and

eventual cell death [26]. ROS generation has been shown to play an important role in apoptosis induced by treatment with AgNPs [27]. The production of reactive oxygen species (ROS) has also been implicated to DNA damage caused by AgNPs, which was reported in a number of in vitro studies [28, 29].

However, there is significant scope for more works in this area, especially the comparative analysis on cytotoxic and genotoxic effects of silver and gold nanomaterials on cancer cell lines. Accordingly, this study presents a comparative in vitro evaluation of the effect of AgNPs and AuNPs on the cancer cell lines such as A549 (Human lung carcinoma), MDA-MB (Human adenocarcinoma mammary gland) and LNCap-FGC (Human carcinoma Prostate). Thus, the new therapeutic agents needed should be more active, produce fewer side effects and act through a unique mechanism, compared to the existing cytotoxic agents. The nanoparticles were synthesized by using *Cassia auriculata* leaf extract at room temperature, and characterized by techniques such as UV–Vis spectroscopy, Fourier Transform Infrared (FTIR) spectroscopy, X-ray diffraction (XRD) and Transmission Electron Measurement (TEM).

Materials and Methods

Materials

All chemical agents including chloroauric acid (HAuCl4) and silver nitrate (AgNO$_3$) were obtained from Himedia, Bangalore. The cancer cell lines such as A549 (Human lung carcinoma), MDA-MB (Human adenocarcinoma mammary gland), LNCap-FGC (Human carcinoma Prostate) were purchased from National Center for Cell Sciences (NCCS, Pune India), and was maintained in Dulbecco's modified Eagle's medium supplemented with 10 % fetal bovine serum (FBS) and 1 % antibiotic solution.

Biosynthesis

Freshly prepared double-distilled water was used throughout the experiments. For the biosynthesis of gold and silver nanoparticles, 10 ml of *C. auriculata* leaf extracts is mixed with 100 ml of 1 mM AgNO$_3$ and 1 mM HAuCl$_4$ solution separately in 250 ml conical flask at room temperature. The solution started changing color within 3 min for characteristic ruby-red for gold and 10 min from yellow to dark brown for silver.

UV–Vis Spectroscopy

Small aliquot of gold and silver nanoparticles solution was used for UV–Vis spectroscopy. The measurement was carried out on a JASCO dual-beam spectro-photometer (model V-570) operated at a resolution of 1 nm. FTIR measurements were carried out on a Perkin-Elmer (Model-783) in the diffuse reflectance mode operating at a resolution of 4 cm^{-1}. After complete reduction of gold and silver ions

by the *C. auriculata* leaf broth, the solutions of gold and silver nanoparticles were centrifuged at 5,000 rpm for 20 min to isolate the gold and silver nanoparticles from free proteins or other compounds present in the solution. The nanoparticle pellets obtained after centrifugation were redispersed in water and centrifuged 3 times to get nanoparticles free from traces of free proteins or other compounds present in the solution.

X-ray Diffraction (XRD)

XRD measurements of the bioreduced nanoparticles drop coated on glass were done on a powder X-ray diffractometer (PXRD-6000 SCHIMADZU) in the angle range of 10–80 °C at 2θ, scan axis: 2:1 sym. The crystallite domain size was calculated from the width of the XRD peaks using the Scherrer formula as given by:

$$\langle D \rangle = \frac{0.9\lambda}{\beta \cos \theta} \tag{1}$$

where $\langle D \rangle$ is average crystallite size, β indicates the line broadening value of the full width at half maximum (FWHM) of peak, λ is wavelength of irradiated X-rays, and θ is maximum peak position value.

Transmission Electron Measurement (TEM)

TEM measurements were performed on a JEOL model 1200EX instrument operated at an accelerating voltage of 80 kV. The TEM samples of the gold and silver nanoparticles synthesized by the biological reduction were prepared by placing a drop over carbon coated copper grids and allowing the solvent to evaporate.

In Vitro Cytotoxic Activity

The effect of gold and silver nanoparticles on the viability of A549, LNCap-FGC, MDA-MB was determined by MTT (3-[4, 5-dimethylthiazol-2-yl]-2,5-diphenyltet-razolium bromide) assay, based on the reduction of yellow tetrazolium salt by mitochondrial dehydrogenase of metabolically active viable cells to a blue-purple formazan that could be measured spectrophotometrically. Hence, the intensity of the color in the solution is directly proportional to cell viability. Cells were cultured in Dubelco's modified essential medium (DMEM) with 10 % fetal bovine serum containing penicillin (100 units/ml) and streptomycin (100 μg/ml). In all the experiments, cells were maintained at 37 °C in a humidified 5 % CO_2 incubator. A549, LNCap-FGC, MDA-MB cells at the concentration of 1×10^6 cells/ml were taken into 96 well plates. Then, the cells were treated with different concentrations of AuNPs and AgNPs (10, 20 and 30 μg/ml) and incubated for 4 h in the presence of 5 % CO_2 and 95 % humidity at 37 °C by adding MTT (100 μl). The formazan crystals were dissolved in 100 μl of DMSO and the absorbance of wells containing cells and blank was measured at 490 nm. The absorbance values of the test (treated) and control (untreated) cells were used for the determination of the percentage cell

viability. Cell survival in control cells was assumed to be 100 %. The percentage cell viability was calculated by formula:

$$\% \, \text{Cell viability} = \frac{\text{O.D. of test} \times 100}{\text{O.D. of control}} \tag{2}$$

DNA Fragmentation Assay

A549, LNCap-FGC, MDA-MB (10^6 cells mL) were seeded in 6-well Microplates and treated with 10, 20 and 30 μg/mL of AuNPs and AgNPs. After 24 h of treatment, the culture medium was removed, and the cells were harvested by scraping with 1 mL of PBS and lysed with 500 μL of lysis buffer [20 mM Tris–HCl (pH 8.0), 5 mM EDTA, 400 mM NaCl, 1 % SDS, and 10 mg/mL proteinase K] for 1 h at 55 °C. Fragmented DNA was extracted with phenol/chloroform/isoamyl alcohol (25:24:1 v/v/v), precipitated with ethanol, and resuspended in Tris–EDTA buffer (TE, pH 8.0) containing 20 μg/mL RNase A. For quantitative analyses of DNA content, an equal amount of DNA was loaded and run on a 1.0 % agarose gel containing 1 μg/mL ethidium bromide at 70 V, and the DNA fragments were visualized by exposing the gel to ultraviolet light, followed by photography.

Results and Discussion

The aim of the study was to describe biosynthesis and characterization of gold and silver nanoparticles using leaf extract and to observe dose dependent cytotoxicity and genotoxicity of gold and silver NPs on A549, LNCap-FGC, MDA-MB. The half maximal inhibitory concentration (IC50) was calculated as the concentration required for inhibiting the growth of cancer cells in culture by 50 % compared to the untreated cells. It has been reported that medicinally valuable angiosperms have the greatest potential for the synthesis of metallic nanoparticles with respect to quality and quantity [30]. The formation of pure metallic nanoparticles and bimetallic nanoparticles by reduction of the metal ions was possibly facilitated by reducing sugars or terpenoids [31]. Nanoparticles with the size range between 1 and 1,000 nm mainly explored for the diagnosis and treatment of human cancers which led to the new discipline of nano-oncology [32].

UV–Vis Spectroscopy

The gold and silver NPs were prepared in 1 mM aqueous solution by reducing HAuCl$_4$ and AgNO$_3$. As the plant extract was mixed in the aqueous solution of ion complex, the color started changing from ruby red to brown due to reduction of ions and excitation of surface plasmon vibrations, which indicate the formation nanoparticles [33]. The UV visible spectra of the synthesized nanoparticles was 523 in gold and 421 nm in silver NPs (Fig. 1).
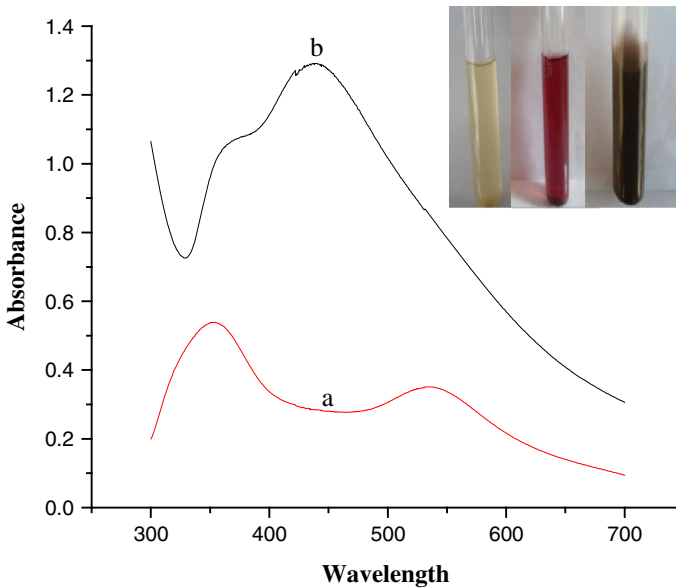
Fig. 1 UV–Vis absorption spectra of nanoparticles *a* Gold *b* Silver

FTIR Analysis

FTIR spectra shows various functional groups present at various positions as shown in Fig. 2. The important characteristic peaks found for carbonyl group of amino acid residues. Peptides of proteins possess strong ability to stick on metals so that the proteins form a coating over the nanoparticles (capping of AgNP/AuNP). This prevents agglomeration of the particles, and thus the nanoparticles are stabilized in the medium. The peaks in the region between 3,292 to 1,599 and 1,066 cm^{-1} are assigned to stretching of N–H, O–H and C=O of primary and secondary amides. The binding of amines of proteins on gold nanoparticles during *Cinnamomum zeylanicum* mediated synthesis was reported [34]. The presence of important phytochemicals [35] and essential amino acids [36] in *C. auriculata* might have facilitated the synthesis and stabilization of nanoparticles. The FTIR analysis reveals the dual function of biological molecules, which might contribute to the reduction and stabilization of gold and silver nanoparticles in the aqueous medium.

XRD Analysis

The XRD patterns obtained for the gold nanoparticles and silver nanoparticles show a number of Bragg reflections corresponding to (111), (200) and (210) in gold, and (111), (221) and (110) in silver. Sets of lattice planes observed which may be indexed based on the structure of metal nanoparticles (Fig. 3). The average particle sizes obtained were 21 nm in gold and 20 nm in silver. The XRD pattern thus clearly shows crystalline nature of gold and silver nanoparticles.
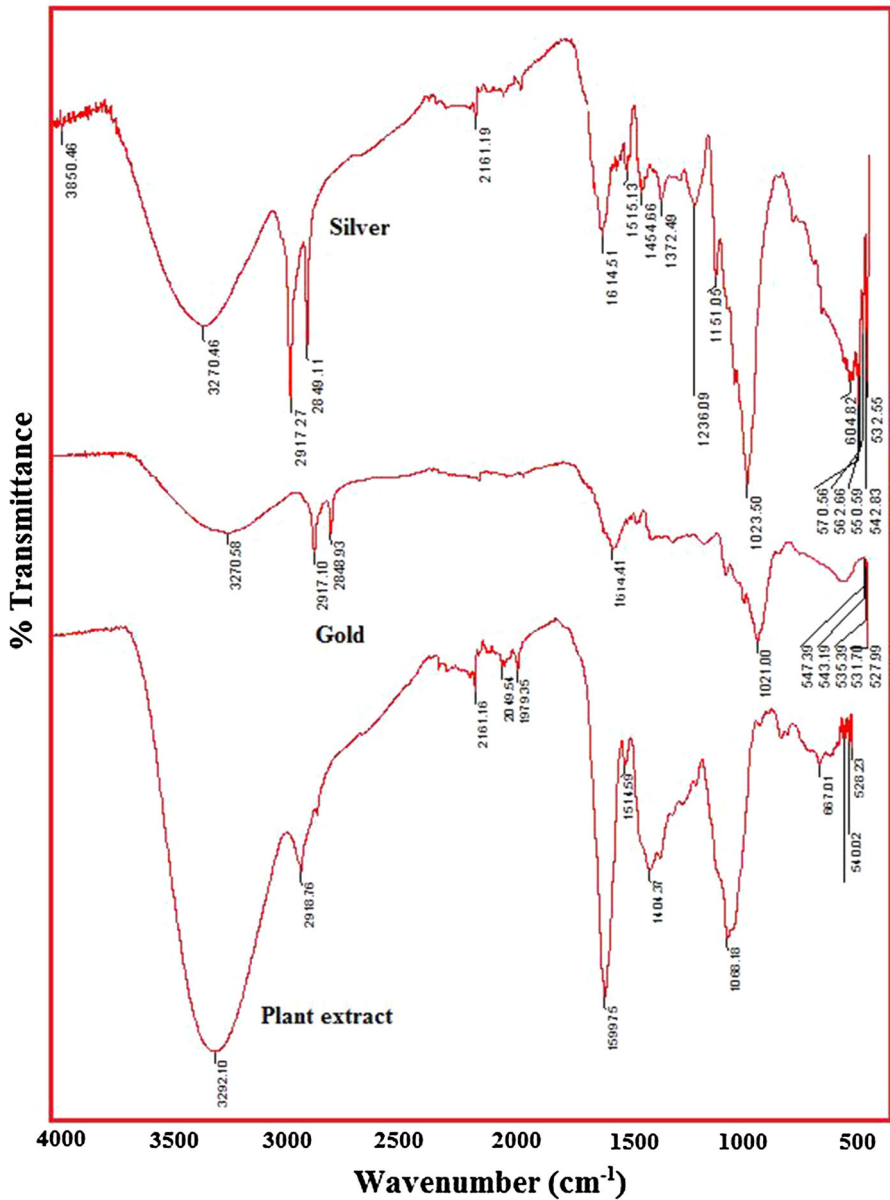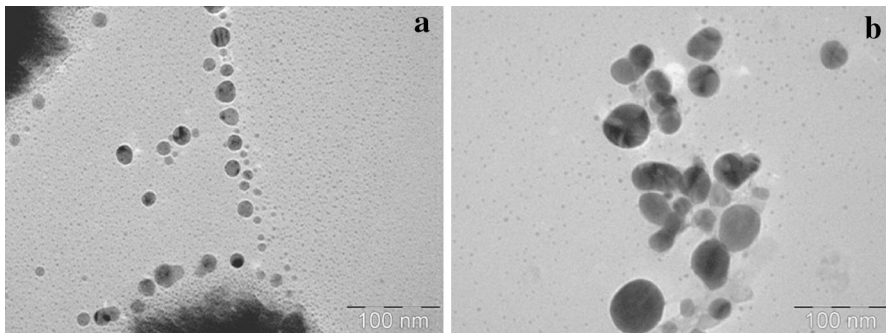
Fig. 2 FTIR spectra of *Cassia auriculata* Leaf extract, *Gold* and *Silver* nanoparticles

TEM Analysis

TEM micrographs of the synthesized Au and Ag nanoparticles were polydispersed and spherical in shape (Fig. 4a, b).
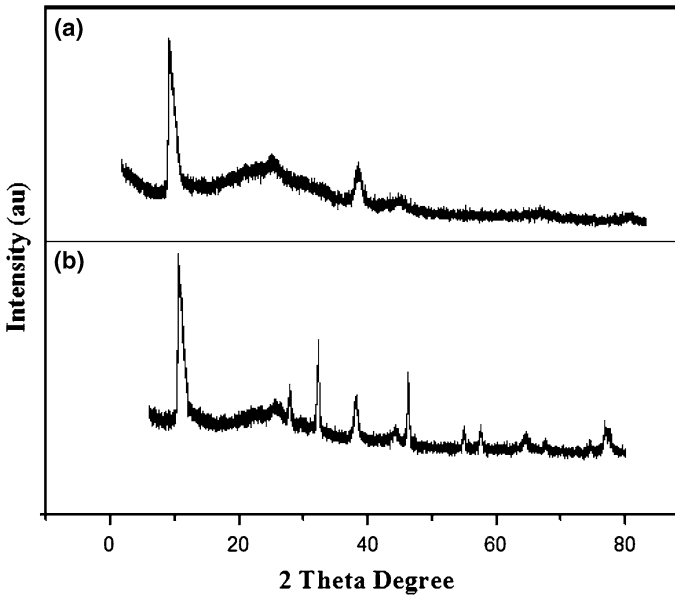
Fig. 3 XRD pattern of nanoparticles **a** Gold **b** Silver

Fig. 4 Transmission electron micrograph of nanoparticles **a** Gold **b** Silver

Cytotoxicity

The effect of synthesized AuNPs and AgNPs on human carcinoma cell lines were determined by knowing IC50 values using MTT assay (Fig. 5a–c). The IC50 of AuNPs was obtained at 10 µg/ml on all the cancer cell lines and increased concentration of AuNPs 30 µg/ml resulted in 100 % cell lysis. The IC50 for AgNPs could be less than 10 µg/ml, as this concentration has resulted in 100 % cell lysis of cancer cell lines (Fig. 6a–c). Longer exposures could result in additional toxicity to the cells. These results demonstrate that AuNPs and AgNPs mediate concentration-dependent increase in toxicity. However, the actions of AuNPs and AgNPs depend

on size, shape, conditions of media, type of cells, dose and exposure time. Since most nanotoxicological screening studies found simpler to perform in in vitro on cell cultures. Even though results may not accurately predict the in vivo toxicity [37] they provide a basis for understanding the mechanism of toxicity and nanoparticle uptake at the cellular level. Several studies have demonstrated that the AuNPs are biologically inert and non-toxic [38]. The cytotoxicity induced by gold nanoparticles depends on size, shape, functional group, charge as well as on the method of cellular uptake [39]. It was found that 1.4-nm gold nanospheres triggered necrosis, mitochondrial damage and oxidative stress on all examined cell lines, and found no evidence of cellular damage for 15 nm gold nanospheres bearing the same surface group [40]. The result highlights the possible size dependent toxicity of gold nanoparticles, while many studies focused on determining the lethal dosage of nanoparticles (LD50, dose required to kill half of the population). In addition, the potential cytotoxicity of AgNPs against cancer was demonstrated [41]. The effect of colloidal silver on MCF7 human breast cancer cells was also reported [42]. AgNPs, disrupts normal cellular function, affects the membrane integrity and induces various apoptotic signaling genes of mammalian cells leading to programmed cell death [43]. The IC50 value and molecular mechanism of 10–15 nm size of AgNPs mediated cytotoxicity in BHK21 (noncancer) and HT29 (cancer) cells observed to be 27 µg/ml [44], whereas in our study IC50 value was lesser than the concentration reported. The present IC50 results revealed that *C. auriculata* mediated synthesized AgNPs shows more efficacy than the previous report. In a study on the effects of AgNPs on skin using the human derived keratinocyte HaCaT cell line model, AgNPs caused a concentration and time-dependent decrease of cell viability, with IC50 values of $6.8 \pm 1.\mu M$ (MTT assay) and $12 \pm 1.2\ \mu M$ (SRB assay) after 7 days of contact [45], however in our experiment the incubation time of cell with nanoparticles was only 4 h which have revealed 100 % cell lysis in short period of time and made these nanoparticles more efficient. Using an MTT assay, comparison of effective concentration (EC50) values of AgNPs of different sizes (~ 5 nm, ~ 20 nm, and ~ 50 nm) and surface areas on different cell types (A549, HepG2, MCF-7, and SGC-7901 cells) were also evaluated [46]. The silver nanoparticles on Human Epidermoid Larynx Carcinoma cell line exhibited a dose-dependent toxicity, and the viability of Hep-2 cells was decreased to 50 % (IC50) at the concentration of 500 nM [21]. In the present study silver nanoparticles were found to be more toxic than gold nanoparticles as also reported earlier [47]. The flavonoid-conjugated AgNPs were devoid of anticancer effect and found synergic effect of AuNPs on cell lines [20], lower cytotoxicity of AgNPs compared to AuNPs may attributed to the difference in surface charges between NPs [48]. The cytotoxic effects of silver nanoparticles were due to active physicochemical interaction of silver atoms with the functional groups of intracellular proteins, as well as with the nitrogen bases and phosphate groups in DNA [49].

DNA Fragmentation

This assay involves extraction of DNA from a lysed cell homogenate followed by agarose gel electrophoresis. We examined the impact of AuNPs and AgNPs in DNA
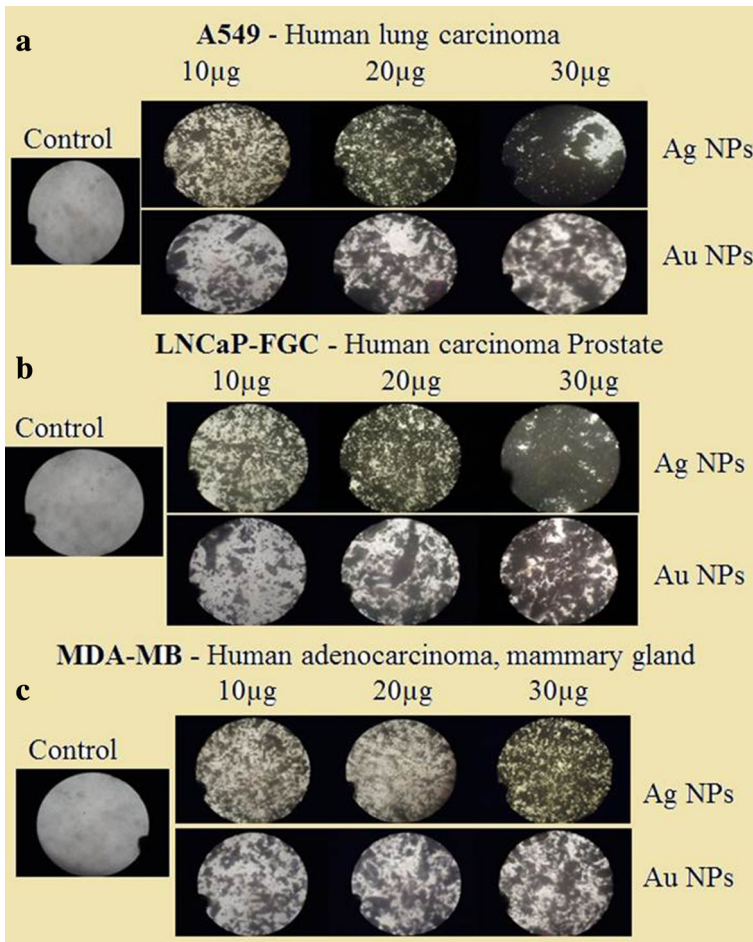
Fig. 5 Microscopic image showing the anticancer effect of AuNP and AgNP synthesized using aqueous extracts of *Cassia auriculata* leaf, at different concentrations **a** A549 **b** LNCap-FGC **c** MDA-MB

fragmentation. The gel after electrophoresis clearly reveals that the intensity of all treated DNA samples has diminished, possibly because of the cleavage of the DNA (Fig. 7). The metals produce ROS such as hydroxyl radical (OH), superoxide radical (O^{2-}) or hydrogen peroxide (H_2O_2) which cleaves the DNA. These nanoparticles produce oxidative stress which causes direct damage to the DNA in which a single electron may be accepted or donated by the metal. Excessive production of ROS in the cell known to induce apoptosis [50] and plays an important role in apoptosis induced by AgNPs [51]. AgNPs were also reported to induce severe structural damage and accumulate in mitochondria, which eventually contributes to oxidative stress [28]. Generation of excessive intracellular ROS leads to apoptosis and necrosis [52] because increased ROS levels correlate with massive DNA breakage and high levels of apoptosis and necrosis [53]. However a number of mechanisms

Fig. 6 Graphical presentation showing the anticancer effect of AuNP and AgNP synthesized using aqueous extracts of *Cassia auriculata* leaf, at different concentrations **a** A549 **b** LNCap-FGC **c** MDA-MB
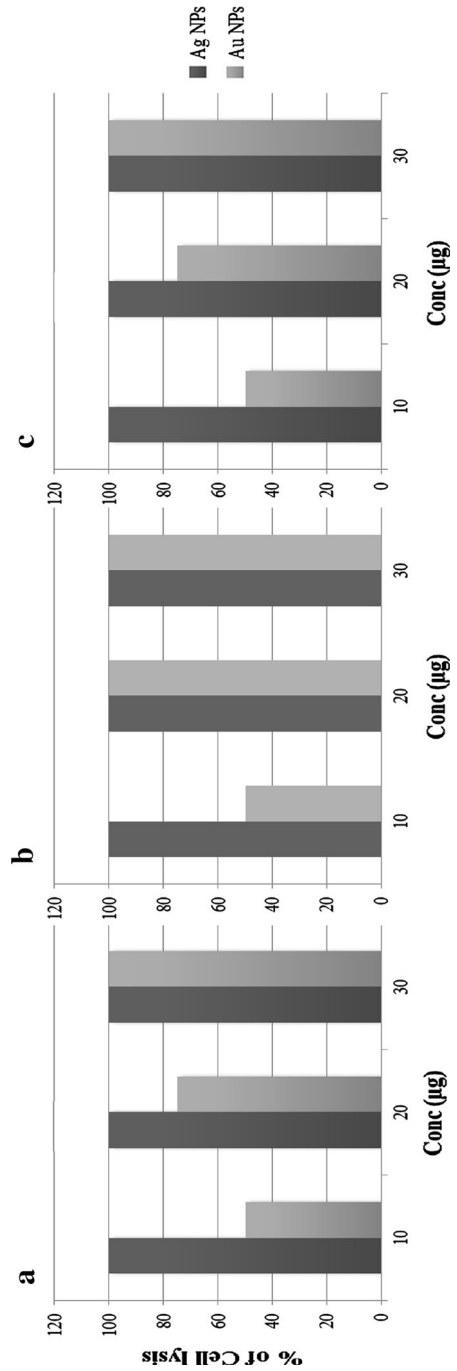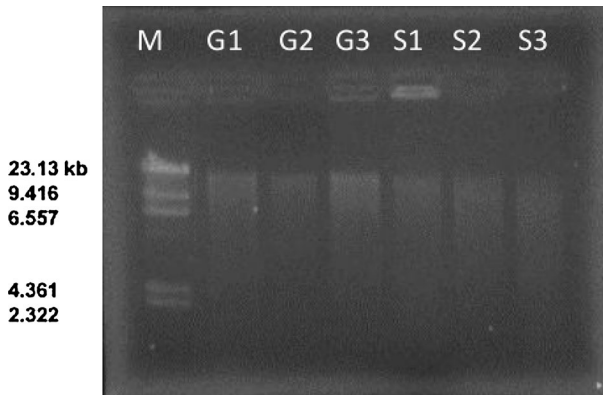
Fig. 7 DNA cleavage activity of Au and Ag nanoparticles (*M* Standard DNA), *G* (Gold NPs), *S* (Silver NPs) (1–10 µg/ml, 2–20 µg/ml, 3–30 µg/ml)

affect the ability of nanoparticles to cause DNA damage. ROS may cause DNA–protein crosslinks, damage to the deoxyribose phosphate backbone, and specific chemical modifications of purine and pyrimidine bases [54]. ROS can also modify the DNA bases and cause strand scission by degrading the ribose ring [55]. The DNA damage by gold nanoparticles further supports the fact that gold nanoparticles induced apoptosis in HL-60 cells [23]. Highly reactive ROS caused oxidative harm to DNA and cell enzymes [56]. Panda et al. 2011 [57] suggested that AgNPs induced DNA damage was apparently mediated through ROS. It was reported that H_2O_2 being highly reactive with Ag, yielded OH radicals which in turn damaged DNA [58, 59].

Conclusion

This study has analyzed the cytotoxicity and genotoxicity of *C. auriculata*-mediated gold and silver nanoparticles against cancer cell lines. The hypothesis of this study, that cell killing could be the possible mechanism induced by the cytotoxic effect of biosynthesized gold and silver nanoparticle was proved, as the growth of the cells was observed to be inhibited. However, further study is needed to understand the exact mechanism of anticancer activity of these nanoparticles. Based on MTT assay, AgNPs less than 10 µg/ml revealed 100 % cell lysis whereas IC50 of AuNPs was 10 µg/ml in all tested cell lines. Therefore, it can be concluded that biologically synthesized AgNPs and AuNPs has promising anticancer effect where AgNPs are more toxic than AuNPs and can be further manipulated for potential biomedical applications. However, the exact mechanism behind the anticancer effects of these nanoparticles needs to be studied.

References

1. R. Siegel, D. Naishadham, and A. Jemal (2012). *Cancer J. Clin.* **62**, 10.
2. World Health Organization (2012) Available at: http://www.who.int/mediacenter/factsheets/fs297/en/index/html. Accessed November 7.
3. A. Kotnis, R. Sarin, and R. Mulherkar (2005). *J. Biosci.* **30**, 93.
4. A. Jemal, R. Siegel, E. Ward, T. Murray, J. Xu, and M. J. Thun (2007). *Cancer J. Clin.* **57**, 43.
5. F. Brayand and B. Moller (2006). *Nat. Rev. Cancer.* **6**, 63.
6. M. M. Gottesman, T. Fojo, and S. E. Bates (2002). *Nat. Rev. Cancer.* **2**, 48.
7. A. L. Harris and D. Hochhauser (1992). *Acta Oncol.* **31**, 205.
8. L. Zhang, F. X. Gu, J. M. Chan, A. Z. Wang, R. S. Langer, and O. C. Farokhzad (2008). *Clin. Pharmacol. Ther.* **83**, 761.
9. V. Wagner, A. Dullaart, A. K. Bock, and A. Zweck (2006). *Nat. Biotechnol.* **24**, 1211.
10. N. J. Farrer, L. Salassa, and P. J. Sadler (2009). *Dalton. Trans.* **48**, 10690. [PubMed: 20023896].
11. Y. Unno, Y. Shino, F. Kondo, N. Igarashi, et al. (2005). *Clin. Cancer. Res.* **11**, 4553.
12. S. A. Abraham, C. McKenzie, D. Masin, T. O. Harasym, L. D. Mayer, and M. B. Bally (2004). *J. Clin. Cancer. Res.* **10**, 728.
13. J. C. Byrd, D. M. Lucas, A. P. Mone, J. B. Kitner, J. J. Drabick, and M. R. Grever (2000). *J. Hematol.* **101**, 4547.
14. T. J. Webster (2006). *Int. J. Nanomedicine.* **1**, 373.
15. D. Prabhu, C. Arulvasu, G. Babu, R. Manikandan, and P. Srinivasan (2013). *Process Biochem.* **48**, 317.
16. M. Jeyaraj, G. Sathishkumar, G. Sivanandhan, D. MubarakAli, M. A. R. Rajesh, G. Kapildev, M. Manickavasagam, N. Thajuddin, K. Premkumar, and A. Ganapathi (2013). *Colloids Surf. B Biointerfaces.* **106**, 86.
17. K. Satyavani, S. Gurudeeban, T. Ramanathan, and T. Balasubramanian (2011). *J. Nanobiotechnol.* **9**, 43.
18. R. Govender, A. Phulukdaree, R. M. Gengan, K. Anand, and A. A. Chuturgoon (2013). *J. Nanobiotechnol.* **11**, 5.
19. S. Lokina and V. Narayanan (2013). *Chem. Sci. Trans.* **2**, 105. doi:10.7598/cst2013.22.
20. D. Raghunandan, B. Ravishankar, S. Ganachari, B. Mahesh, et al. (2011). *Cancer Nanotechnol.* **2**, 57. doi:10.1007/s12645-011-0014-8.
21. S. Kaliyamurthi, G. Selvaraj, R. Thiruganasambandam, and B. Thangavel (2012). *Avicenna J. Med. Biotechnol.* **4**, 35.
22. M. S. Ghassan, H. M. Wasnaa, R. M. Thorria, et al. (2013). *Asian Pac. J. Trop. Biomed.* **3**, 58.
23. R. Geetha, T. Ashokkumar, S. Tamilselvan, K. Govindaraju, M. Sadiq, and G. Singaravelu (2013). *Cancer Nanotechnol.* **4**, 91. doi:10.1007/s12645-013-0040-9.
24. M. Jannathul Firdhouse and P. Lalitha (2013). *Cancer Nanotechnol.* **4**, 137. doi:10.1007/s12645-013-0045-4.
25. A. Nan, X. Bai, S. J. Son, S. B. Lee, and H. Ghandehari (2008). *Nano Lett.* **8**, 2150.
26. S. H. Kim, H. S. Lee, D. S. Ryu, et al. (2011). *Korean J. Microbiol. Biotechnol.* **39**, 77.
27. C. Carlson, S. M. Hussein, A. M. Schrand, et al. (2008). *J. Phys. Chem.* **112**, 13608.
28. P. V. Asharani, G. L. K. Mun, M. P. Hande, and S. Valiyaveettil (2009). *ACS Nano.* **3**, 279.
29. R. Foldbjerg, P. Olesen, M. Hougaard, D. A. Dang, H. J. Hoffmann, and H. Autrup (2009). *Toxicol. Lett.* **190**, 156.
30. S. K. Kumar and J. Yadav (2009). *Chem. Technol. Biotechnol.* **84**, 151.
31. S. ShivShankar, R. Akhilesh, A. Absar, and S. Murali (2004). *J. Colloid Interface Sci.* **275**, 496.
32. M. V. Yezhelyev, X. Gao, Y. Xing, A. Al-Hajj, S. Nie, and R. M. O'Regan (2006). *Lancet Oncol.* **7**, 657.
33. P. K. Jain, K. S. Lee, I. H. El-Sayed, and M. A. El-Sayed (2006). *J. Phys. Chem. B* **110**, 7238.
34. S. L. Smitha, D. Philip, and K. G. Gopchandran (2009). Spectrochim. *Acta Part A Mol. Biomol. Spectrosc.* **74**, 735.
35. V. Usha and A. K. Bopaiah (2012). *Int. J. Pharm. Bio. Sci.* **3**, 260.
36. S. A. Gaikwad, K. Asha, M. Kavita, N. R. Deshpande, and J. P. Salveka (2010). *Int. J. Pharm. Tech. Res.* **2**, 1092.
37. L. G. Griffith and M. A. Swartz (2006). *Nat. Rev. Mol. Cell Biol.* **7**, 211. doi:10.1038/nrm1858.

38. C. M. Goodman, C. D. McCusker, T. Yilmaz, and V. M. Rotello (2004). *Bioconjug. Chem.* **15**, 897. doi:10.1021/bc049951i.
39. Y. S. Chen, Y. C. Hung, I. Liau, and G. S. Huang (2009). *Nanoscale Res. Lett.* **4**, 858. doi:10.1007/s11671-009-9334-6.
40. Y. Pan, A. Leifert, D. Ruau, and S. Neuss (2009). *Small.* **5**, 2067. doi:10.1002/smll.200900466.
41. M. I. Sriram, S. B. M. Kanth, K. Kalishwaralal, and S. Gurunathan (2010). *Int. J. Nanomedicine.* **5**, 753.
42. M. A. Franco-Molina, E. Mendoza-Gamboa, C. A. Sierra-Rivera, et al. (2010). *J. Exp. Clinical Cancer Res.* **29**, 148.
43. P. Sanpui, A. Chattopadhyay, and S. S. Ghosh (2011). *ACS Appl. Mater. Interfaces.* **3**, 218.
44. P. Gopinath, S. K. Gogoi, A. Chattopadhyay, and S. S. Ghosh (2008). *Nanotechnology.* **19**, Article ID 075104.
45. C. Zanette, M. Pelin, M. Crosera, et al. (2011). *Toxicol. In Vitro.* **25**, 1053.
46. W. Liu, Y. Wu, C. Wang, et al. (2010). *Nanotoxicology.* **4**, 319.
47. R. Foldbjerg, D. A. Dang, and H. Autrup (2011). *Arch. Toxicol.* **85**, 743.
48. H. J. Yen, S. H. Hsu, and C. L. Tsai (2009). *Small.* **5**, 1553.
49. S. Moaddab, H. Ahari, D. Shahbazzadeh, et al. (2011). *Int. J. Nano Lett.* **1**, 11.
50. J. L. Martindale and N. J. Holbrook (2002). *J. Cell. Physiol.* **192**, 1.
51. C. Carlson, S. M. Hussein, A. M. Schrand, et al. (2008). *J. Phys. Chem.* **112**, 13608.
52. S. Hackenberg, A. Scherzed, and M. Kessler (2011). *Toxicol. Lett.* **201**, 27.
53. R. P. Singh and P. Ramarao (2012). *Toxicol. Lett.* **213**, 249.
54. M. Dizdaroglu (1991). *Free. Radic. Biol. Med.* **10**, 225.
55. P. Yang and F. Gao (2002). *Principle of Bioinorganic Chemistry*. Science press, Beijing, pp. 322 (in Chinese).
56. J. Boonstra and J. A. Post (2004). *Gene.* **337**, 1.
57. K. K. Panda, V. M. Achary, R. Krishnaveni, B. K. Padhi, S. N. Sarangi, S. N. Sahu, and B. B. Panda (2011). *Toxicol. In Vitro.* **25**, 1097.
58. N. Lubick (2008). *Environ. Sci. Technol.* **42**, 8617.
59. J. Cadet, T. Douki, and J. L. Ravanat (2010). *Free. Radic. Biol. Med.* **49**, 9.